Journal of Materials Chemistry B

Accepted Manuscript

ROYAL SOCIETY OF CHEMISTRY

www.rsc.org/materialsB

Synthesis and characterization of a novel injectable alginate-collagen-hydroxyapatite hydrogel for bone tissue regeneration

Stephanie T. Bendtsen, Mei Wei*

Department of Materials Science and Engineering, Institute of Material Science, University of Connecticut

97 North Eagleville Rd, Unit 3136, Storrs, CT, 06269

*Corresponding author
Phone: (860) 486-9253
Fax: (860) 486-4745
Email: meiwei@engr.uconn.edu

Abstract

The rigid architecture of implanted scaffolds for bone tissue engineering often provides a limited ability to fill irregular contours of bone defects. Thus, injectable hydrogels are used to completely fill the defects while enhancing bone formation of the area. In this study, an injectable alginate hydrogel with a gelation time ranging from 5-10 minutes was developed by varying the concentrations of phosphate and calcium involved in the gelation process. The incorporation of mineralized collagen fibers within the hydrogel further increased the mechanical properties and osteoconductivity of the hydrogels. The gelation time, dynamic mechanical analysis (DMA) and thermogravimetric analysis (TGA) results suggested that the order in which the phosphate was added to the system had an effect on the gelation mechanism. This was further investigated to find that the addition of phosphate prior to the alginate powder resulted in better control of the gelation time and thus a more uniform hydrogel. The presence of hydroxyapatite in the hydrogels was confirmed using various characterization techniques, including X-ray diffraction (XRD) and Fourier transform infrared spectroscopy (FTIR). This novel fabrication process allowed for the development of an injectable hydrogel system with components necessary for promoting enhanced bone regeneration as well as host-implant integration.

Key words: bone tissue engineering, injectable hydrogel, alginate, collagen, hydroxyapatite

1. Introduction:

Bone tissue engineering scaffolds have been researched extensively in hope to find an ideal construct that is biocompatible, biodegradable, promotes bone regeneration and mimics the distinctive properties of natural bone. It is especially important that the composition closely resembles that of bone and the native extracellular matrix in order to promote favorable cell attachment and proliferation. The main components of natural bone found in the human body include inorganic hydroxyapatite nanocrystals and organic collagen fibrils.[1] The first bone tissue engineered scaffolds aimed to mimic the composition of natural bone and possess regeneration capabilities were developed in the form of calcium phosphate ceramic implants.[2,3] Since then, calcium phosphate cements and scaffolds have been constructed in combination with various biopolymers such as polycaprolactone, chitosan and collagen to produce biocompatible composites capable of promoting bone regeneration. [4-9] Specifically, a well known co-precipitation method first developed by Kikuchi et al. has been followed to fabricate scaffolds in which hydroxyapatite nanocrystals are nucleated onto collagen fibers that precipitate out of solution.[10] Many variations of this self assembling method have since been established.[11,12] Recently, our group has developed a novel co-precipitation method involving the nucleation of apatite onto collagen fibers in a modified simulated body fluid (m-SBF). [13,14] These lyophilized scaffolds have been proven to be biocompatible and promote new bone growth.[15]

Despite the early success in the preparation of lyophilized bone tissue engineering scaffolds, they must be surgically implanted into the bone defect of the patient. Thus, researchers have been gravitating towards the development of novel, non-invasive, injectable hydrogel scaffolds for bone tissue engineering. The current most widely used technique is the use of sol-gel polymerization. Sol-gel mechanisms include photopolymerization, thermogelation,

concentration dependent chemical reactions and various additional mechanisms.[16-18] Photopolymerization techniques involve the radical chain polymerization of a polymer in which an acrylic or methacrylic side group is initiated and polymerized by a photoinitiator (I2959) under UV light.[17] Similarly, many thermogelation techniques involve the monomeric polymerization of polymers with non-degradable backbones such as pNiPAAm based polymers which introduce side groups that are potential cytotoxic agents.[19,20] This possibility of cytotoxicity and additional adverse immune responses render these polymer modification processes less biocompatible for injectable hydrogel purposes. Thus, injectable systems without polymeric modification such as ionically crosslinked systems are more suitable.

An extensively researched ionically crosslinked injectable hydrogel system includes the use of the naturally occurring polysaccharide alginate, produced by brown algae such as macrocystis pyrifera (kelp).[21] Applications in which alginate is used range from food stabilizers in ice cream to biomedical applications such as dental molds, wound dressings, cell immobilization, drug delivery and bone tissue engineered scaffolds.[22-25] Alginate is a linear co-polymer composed of consecutive blocks of (1-4) linked α-L-guluronate (G-blocks) and β-D-mannuronate (M-blocks) followed by segments of alternating MG blocks.[26] Grant et al. first described the formation of an "egg box structure" as a result of the G blocks in the presence of divalent cations such as calcium, barium and strontium.[27] The divalent cations form intermolecular bonds with two deprotonated carboxylate groups of one G block and with two hydroxyl groups of another.[28] The β glycolic linkage of the M blocks has a low affinity for divalent cations, resulting in weak interactions. The G blocks are therefore most significant in the crosslinking process.[29] As a result of this crosslinking of lateral egg box multimers, the alginate undergoes a sol-gel transition.[18]

Martinsen et al. found that the sol-gel transition occurs instantaneously to form alginate gel microspheres when alginate is added dropwise to a calcium chloride solution.[23] Although this property may be favorable for some applications such as cell immobilization, the fast gelation rate may not be ideal for others, such as injectable purposes.[24] Cho et al. proposed the use of $CaSO_4$ as a gelling agent and Na_2HPO_4 as a retardation agent to control the gelation rate of an alginate gel.[30] Controlling the gelation rate allows for homogenous gel formation and uniform material properties.[31]

Unfortunately, alginate on its own has shown to induce reduced cell attachment *in vitro* due to its hydrophilic and negatively charged properties as well as poor osteoconductivity.[26] Therefore researchers have expanded to using combinations of alginate with more biocompatible components such as PVA, hydroxyapatite, collagen and chitosan.[30,32-35] Particularly, the combination of alginate, collagen and hydroxyapatite has been extensively researched. [25,35-37] Commonly, pre-fabricated, lyophilized collagen-apatite powder is added to an alginate suspension which is then gelled and lyophilized for further characterization. *In vitro* studies have shown that the addition of collagen and hydroxyapatite to the alginate hydrogel provided a favorable environment for osteoblast attachment and proliferation.[37]

Thus, the focus of our work is developing a novel combination of an injectable alginate-collagen hydrogel with *in situ* hydroxyapatite nucleation onto collagen fibers. This combination provides appropriate mechanical strength as a bone tissue substitute and the components necessary to promote bone regeneration without lyophilization, proving its potential for an injectable regenerative material.

2. Materials and Methods:

2.1 Preparation of hydrogels

2.1.1 Preparation of alginate hydrogels

Alginic acid sodium salt (medium viscosity; MP Biomedicals LLC, USA) was added to 6 mL of deionized water in polystyrene vials (25.9 mL; ID x H: 26 x 51 mm) and mixed with 2 mL of sodium phosphate dibasic anhydrous (Na_2HPO_4, ≥ 99%, Fisher Scientific, USA) solutions at varying concentrations according to Table 1. The suspensions then sat for 1 hour at room temperature before 8 mL of calcium sulfate anhydrous ($CaSO_4$, 99%, Alfa Aesar, USA) solutions of varying concentrations were added and mixed for 30 seconds. The gelation time was observed and recorded as defined by the test tube tilting method.[31] Briefly, the vial was tilted 90° every minute after initial mixing and the time at which the meniscus of the suspension no longer moved was designated as the gelation point. As shown in Table I, the final weight percent of alginate was 1.5 % (w/v) while the final weight percentages of Na_2HPO_4 and $CaSO_4$ ranged from 0-0.12 % (w/v) and 0.2-0.40 % (w/v), respectively. Alginate hydrogels with 0.12 % (w/v) P (Na_2HPO_4) and 0.40 % (w/v) Ca ($CaSO_4$) were chosen for the addition of collagen fibers and mineralized collagen fibers.

After the gelation test, A-P-4, A-P-5 and A-P-9 hydrogels were chosen to proceed with mechanical testing as their gelation times fell in the range of 5-30 minutes, defined as ideal in a surgical setting.[3] The A-Ca-1 hydrogel was selected to act as the control.

2.1.2 Preparation of alginate-collagen (A-C) hydrogels

Type I collagen was extracted from rat tails following a protocol by Rajan et al.[38] Briefly, the collagen was extracted and dissolved in 0.02 M acetic acid at 4 °C. The pH of the collagen solution was raised to 7 using sodium hydroxide. 30 mL of the collagen solution with a

concentration of 4.5 mg/mL was then covered placed in a waterbath at 37 °C for 24 hours at constant stirring using a magnetic stir bar and stir plate. The precipitates were then collected via filtration and rinsed with deionized water. The fibers were then allowed to air dry for 1 hour. A small amount of fibers were air dried overnight and imaged using FESEM to observe the morphology.

Final compositions of the A-C hydrogels can be seen in Table 2. Collagen fibers were added at 2.5, 5.0, 10.0 and 20.0 % (w/v) to alginate solutions and mixed until homogenously distributed throughout the alginate solutions. Na_2HPO_4 solution was added to the mixture after 20 minutes at 0.12 % (w/v) of the final hydrogel. After 1 hour, $CaSO_4$ solution of 0.40 % (w/v) of the final hydrogel volume was added and the gelation time was recorded as previously described.

2.1.3 Preparation of alginate-mineralized collagen (A-MC) hydrogels

Alginate-mineralized collagen (A-MC) hydrogels were composed of alginate, mineralized collagen fibers, Na_2HPO_4 and $CaSO_4$. A-MC hydrogels differed in the order in which the remaining components were added to the mineralized collagen fiber suspension. A-MC-1 hydrogels were prepared by adding alginate powder prior to the phosphate solution addition whereas for A-MC-2 hydrogels, the phosphate solution was added prior to the alginate powder.

To prepare mineralized collagen fibers, a solution of modified simulated body fluid (m-SBF) was used as the source to provide calcium and phosphate ions.[13,15] Briefly, SBF is composed of inorganic ions similar to the natural composition of human blood plasma. The modified SBF contains ion concentrations 3 times that of normal SBF to ensure mineralization of

collagen fibers. The first two salts in the m-SBF recipe were dissolved in 20 mL of deionized water. A collagen solution of concentration 4.5 mg/mL was then added to the solution and mixed on ice for 10 minutes. The next 3 salts were added to 10 mL of deionized in order after the complete dissolution of the previous ion. This solution was then added to the collagen solution containing the first two ions, which remained on ice, and mixed for an additional 10 minutes. The sodium bicarbonate was added to the collagen-SBF solution and mixed until completely dissolved. The pH of the solution was raised to 7 using sodium hydroxide. The collagen-SBF solution was then added to a waterbath at 37 °C under moderate stirring for 1.5 hours. The stir bar was then removed and the suspension was aged at 37 °C overnight. After 24 hours, the mineralized collagen fiber precipitates were collected via filtration, rinsed twice with deionized water and allowed to air dry. The fibers were weighed at 2.5 and 5 % (w/v) of the final hydrogel. The fibers were re-suspended in 6 mL of deionized water under moderate stirring to re-disperse them in the suspension. 0.24 g alginate powder was then added to the collagen suspension and mixed to form a homogenous suspension. 0.12 % (w/v) P and 0.40 % (w/v) Ca solutions were then added as previously described. The final A-MC-1 hydrogel compositions can be seen in Table 2. The gelation time was recorded according to the test tube tilting method as previously described.

To further investigate gelation properties, A-MC-2 hydrogels (2.5 % w/v) were prepared. Mineralized collagen fibers, prepared as previously described, were added to deionized water followed by an addition of the phosphate solution at 0.12 % (w/v) of the final hydrogel. Alginate powder was then added to the solution at a final concentration of 1.5 % (w/v). $CaSO_4$ at 0.40 % (w/v) final concentration was added and gelation proceeded as previously described.

2.2 Characterization

The morphology of collagen fibers and mineralized collagen fibers were observed using field emission scanning electron microscopy (FESEM) at an accelerating voltage of 5 kV. (FESEM, JEOL JSM-6335F, Japan).

Dynamic mechanical analysis (DMA) was completed using a DMA 2980 Dynamic Mechanical Analyzer (TA instrument Inc., New Castle, DE) in compression mode using 40 mm sandwich fixtures. Pre-determined A-Ca (n=8) and A-P (n=8) hydrogel samples were sliced to an average thickness of 4.5 mm. The hydrogels were loaded into the DMA, ramped to 37°C and held isothermally for 5 minutes. A preload force of 0.01 N was applied, followed by a force ramped up to 18 N at a uniform stress rate of 0.5 N per minute. The compressive modulus was determined from the slope of the initial 20% linear elastic region of the obtained stress-strain curve. The same procedure was implemented for A-C (n=5), A-MC-1 (n=5) and A-MC-2 (n=5) hydrogels.

After DMA testing, remaining hydrogel slices were frozen at -25 °C and lyophilized using a freeze-dryer (Free Zone®, Labconco, USA). The freeze-dried hydrogels of selected compositions, as listed in Table 3, were subjected to a series of evaluations, including thermogravimetric analysis (TGA), X-ray diffraction (XRD), and Fourier transform infrared spectroscopy (FTIR).

TGA was conducted using a TG analyzer (TGA-1000, Rheometric Scientific, UK) to determine the weight percentage of the inorganic components present in the hydrogels. The freeze-dried hydrogels were loaded into the TG analyzer at an average weight of 20 mg. The weight loss profile was recorded from 25 °C to 900 °C in air at a rate of 10 °C per minute and the weight percent residue was determined. X-ray diffraction (XRD, Bruker AXS D5005) was

performed on the freeze-dried hydrogels to determine the composition of the inorganic components present in the hydrogels. Scans were collected over a 2-θ range of 10-50 ° at a step size of 0.02 ° and a scan rate of 0.2 ° per minute with Cu K α radiation (k= 1.54056 nm). FTIR was used to determine the functional groups present in the alginate hydrogels. FTIR spectra were obtained with a Nicolet Magna-IR 560 Spectrometer and a Specac-Onest Single Bounce Diamond ATR Accessory. A small slice of the freeze-dried hydrogel was placed over the diamond and compressed until sufficient contact was made. The spectra were recorded using 32 scans over the range of 400 to 4000 cm^{-1} using OMNIAC software.

2.3 Statistical Analysis

Results were statistically analyzed using one or two-way analysis of variance (ANOVA) and expressed as mean ± standard deviation. Statistical significance was defined as $p < 0.05$.

3. Results

3.1 Gelation Time

The solution and gel states of the alginate are shown in Fig. 1. Average gelation times of alginate hydrogels with varying $CaSO_4$ and Na_2HPO_4 concentrations are shown in Fig. 2. Within groups A-P-1-3 (0.04 % (w/v) Na_2HPO_4) and A-P-7-9 (0.12 % (w/v) Na_2HPO_4), an increase in calcium concentrations resulted in a decrease in gelation time. The slight increase in gelation times seen in groups A-Ca-1-3 (0 % (w/v) Na_2HPO_4) and A-P-4-6 (0.08 % (w/v) Na_2HPO_4) was not statistically significant and the change in gelation times of the hydrogels closely resembled the same trend. Comparing gelation times of alginates composed of the same calcium concentrations displayed an increase in gelation time with increasing Na_2HPO_4 concentration.

Variations from this increase in gelation time were not statistically significant. The control group exhibited variation from the expected increase in gelation time due to the instantaneous, inhomogenous gelation of the alginate chains and hindered diffusion of calcium ions throughout the suspension. The differences in average gelation times of the selected, starred hydrogels were not statistically significant from the control.

Figure 3a) displays a FESEM image of pure collagen fibers added to the alginate hydrogels. The collagen fibers are about 200 nm in width and on the order of micrometers in length. Debanding patterns characteristic of collagen fibers are observed. Figure 3b) shows a FESEM image of mineralized collagen fibers in which apatite particles are deposited along the collagen fibers.

The average gelation times of alginate hydrogels with varying weight percentages of collagen fibers and mineralized fibers are shown in Fig. 4. The addition of collagen fibers at all percentages did not significantly impact the gelation times of the hydrogels when compared to the control. The addition of alginate directly following the mineralized fibers (A-MC-1 hydrogels) resulted in a decrease in average gelation time yet the difference is not statistically significant from the control. However, the average gelation time of A-MC-1 hydrogels (2.5 % w/v and 5 % w/v) did display a statistically significant decrease compared to A-C-1 hydrogels (2.5 % (w/v) pure collagen fibers). When the order of the phosphate addition was modified to be before the alginate (A-MC-2), the gelation time was not significantly different from the control and was slower than those of A-MC-1 hydrogels. A statistically significant difference in gelation time was observed between 5 % (w/v) A-MC-1b and 2.5 % (w/v) A-MC-2 hydrogels.

3.2 Dynamic Mechanical Analysis

The average compressive moduli of alginate hydrogels of varying phosphate and calcium concentrations are shown in Fig. 5. A-Ca-1 hydrogels (0 % (w/v) Na_2HPO_4; 0.20 % (w/v) $CaSO_4$) displayed an average compressive modulus of 1.6 kPa. An increase to 0.08 % (w/v) P and 0.20 % (w/v) Ca increased the average modulus to 2.3 kPa. The addition of 0.08 % (w/v) P and 0.30 % (w/v) Ca increased the average modulus to 3.2 kPa. The average compressive modulus peaked at a value of 5.1 kPa for alginate hydrogels of 0.12 % Na_2HPO_4 and 0.40 % $CaSO_4$, which was significantly higher than the other hydrogels.

The average compression moduli of A-C and A-MC hydrogels are shown in Fig. 6. As a result of the addition of collagen fibers at 2.5, 5 and 10 % (w/v) to alginate hydrogels composed of 0.12 % P and 0.40 % Ca, the compressive moduli of these hydrogels increased significantly. The average compressive modulus peaked at a value of 7.5 kPa for A-C-1 (2.5 % (w/v)) hydrogels. The addition of alginate immediately after the mineralized collagen fibers (A-MC-1) did not result in a statistically significant difference in compressive modulus compared to the control. The modulus of the A-MC-1a (2.5 % (w/v)) hydrogels (6.6 kPa) was significantly lower than that of A-C-2 (5 % (w/v)) hydrogels. The modulus of the A-MC-1b hydrogels (5.9 kPa) was significantly lower than that of both the A-C-1 and A-C-2 hydrogels. When the phosphate solution was added before the alginate (A-MC-2), the modulus reached the maximum of 8.0 kPa. This increased value was statistically significantly different from the original A-MC hydrogels (A-MC-1a and A-MC-1b) and the control.

3.4 Thermogravimetric Analysis

The TGA profiles for alginate hydrogels of various compositions can be seen in Fig. 7.

Decomposition of the alginate hydrogels begins around 26 °C with the loss of water, followed by the rupture of the alginate chains and monomers around 190 °C and 620 °C. The residue includes elements that decompose above 900 °C. The average percent residue for A-Ca-1, A-P-9, A-C-1, A-MC-1a (2.5 % w/v) and A-MC-2 (2.5 % w/v) hydrogels were determined to be 26.8 %, 33.0 %, 32.8 %, 31.4 % and 35.0 %, respectively. The increase in percent residue with the addition of phosphate, collagen fibers or mineralized collagen fibers to the control (A-Ca hydrogel) was statistically significant for all samples. The addition of pure collagen fibers (A-C) or mineralized collagen fibers (A-MC-1) did not result in a statistically significant increase in the percent residue compared to the alginate phosphate hydrogel (A-P-9), nor were they statistically significant from each other. The altered order of the addition of the phosphate solution (A-MC-2) resulted in an increase in residue that was statistically significant from the A-Ca-1, A-C-1 and A-MC-1a hydrogels.

3.3 X-Ray Diffraction

Figure 8 shows x-ray diffraction patterns of A-Ca-1, A-P-9, A-C-1, A-MC-1a and A-MC-2 hydrogels. The A-Ca spectrum depicts characteristic peaks of sodium calcium sulfate hydrate, sodium sulfate and calcium sulfate. The addition of phosphate to the A-Ca hydrogel results in additional peaks of sodium hydrogen phosphate and calcium phosphate carbonate. The addition of collagen fibers to the A-P hydrogels (A-C hydrogels) exhibit peaks characteristic of carbonate apatite around 29° and 32°. The A-MC-1a hydrogel with mineralized collagen fibers displays a greater amount of peaks characteristic of carbonate-hydroxyapatite around 25° and 29° and calcium phosphate carbonate around 19°, 23°, 34° and 38°. The A-MC-2 spectrum displays peaks at the same positions as the A-MC-1a spectra but with increased broadening. Peak broadening

and shifting amongst spectra may be attributed to the overlapping of peaks of the various components of the hydrogels.

3.5 Fourier Transform Infrared Spectroscopy

The FTIR spectra of A-Ca-1 (0.20 % Ca), A-P-9 (0.40 % Ca-0.12 % P), A-C-1 (2.5 % collagen fibers), A-MC-1a (2.5 % mineralized collagen fibers) and A-MC-2 (2.5 % mineralized collagen fibers) hydrogels are shown in Fig. 9. The alginate alone spectrum displays characteristic alginate bands denoting asymmetric and symmetric stretching of $-COO^-$ modes, found at 1595 cm^{-1} and 1410 cm^{-1}, respectively. C-O stretching vibration modes occur at 1080 cm^{-1}; and hydroxyl stretching bands at 3294 cm^{-1}. Bending of the ^-OH group of the carboxyl is depicted at 889 cm^{-1}. With the addition of phosphate, a shift of the $-COO^-$ bands to higher wavelengths is observed. Bending and stretching of the phosphate modes is observed at 611 cm^{-1} and 997 cm^{-1}, respectively. The addition of pure collagen fibers and mineralized collagen fibers also results in a shift of the carboxyl absorption bands to higher wavelengths. Amide absorption bands of the collagen fibers characteristic of C=O and OH stretching, N-H stretching and C-N stretching can be found at 1670 cm^{-1} and 1630 cm^{-1}, 1550 cm^{-1}, and 1200 cm^{-1}, respectively. PO_4 stretching of the *in situ* formed apatite is located at 1200-965 cm^{-1} and 500-600 cm^{-1}. All of these signature peaks of collagen overlap with characteristic peaks of the A-Ca and A-P hydrogel systems.

4. Discussion

4.1 Gelation Time and Mechanical Properties

The ability to tailor the gelation time and strength of alginate hydrogels as desired is one of the greatest incentives for using alginate in a variety of applications. For injectable hydrogels used in bone tissue engineering, it is ideal that the composition can be adjusted so that the gelation rate is slow enough to allow surgical handling yet fast enough for the hydrogel to achieve *in vivo* stability and functionality soon after injection. The optimal gelation time range has been defined as 5-30 minutes.[36]

The variation in gelation time among the alginate hydrogels with different concentrations of sodium phosphate and calcium sulfate exhibits a strong trend as the time increases with an increase in phosphate concentration and decreases with an increase in calcium concentration, as seen in Fig. 2. The control hydrogels gelled immediately in various regions as the calcium sulfate solution was added without the presence of sodium phosphate. This resulted in inhomogeneous hydrogels. It was difficult for the remaining calcium to diffuse through the immediately gelled sections to reach the unreacted alginate, increasing the time for complete gelation of the whole suspension.[31] Kuo et al. suggested that the use of a calcium source with lower solubility in water allows for a more gradual gelation rate and thereby results in a more homogenous gel. This is because that as the calcium particles are less readily released into the solution, they disperse more evenly throughout the medium over time before massive gelation occurs.

Thus, Cho et al. proposed the use of a gelling agent with intermediate solubility, $CaSO_4$, and a retardation agent, Na_2HPO_4, to control the gelation rate of an alginate hydrogel.[30] The mechanism by which Na_2HPO_4 slows down the gelation of alginate is through a chemical reaction with $CaSO_4$, resulting in the formation of calcium phosphate. Due to the sparing solubility of $CaSO_4$, calcium ions are made available in solution over time. As the calcium is released through the suspension as ions, a high concentration of phosphate ions will quickly react

with them to form calcium phosphate precipitates. This precipitation leaves less calcium available in solution for the immediate gelation of alginate. During this period, the rest of the $CaSO_4$ has more time to disperse throughout the alginate suspension. Thus, once all of the phosphate ions have precipitated with calcium ions, the calcium is then made available to crosslink the alginate G blocks via formation of the egg box structure uniformly throughout the suspension. Therefore, the order of stability of calcium in the composite and thus order of formation can be inferred to be calcium phosphate as the most stable, followed by calcium alginate and finally calcium sulfate.[36] The precipitation mechanism is an advantageous addition to the system to help control the gelation rate but the solubility of the calcium source plays a more dominate role. If a retardation agent is used with a highly soluble source, inhomogenous gelation would still occur because the calcium ions would not be evenly distributed throughout the suspension. Only a combination of the two approaches can result in the greatest control of the gelation rate of the alginate as well as the homogeneity of the resulting hydrogel.

Our data shows that the rate of gelation does in fact decrease with increasing phosphate and decreasing calcium concentrations (and vice versa) for an unchanged concentration of alginate, corroborating previous studies.[30,36] An increase in calcium concentration at a constant concentration of phosphate decreases the gelation time as more calcium ions are made available to participate in the crosslinking with the G blocks of the alginate. This also results in an increase in the ultimate hydrogel strength.[23] A lower phosphate concentration will allow the sol-gel transition to occur more rapidly as the calcium phosphate precipitation will be completed more quickly. The result is a decrease in the homogeneity of the hydrogel and thus its mechanical properties.[36] This was also confirmed by our data as the inhomogeneous controls (without phosphate) exhibited the lowest compressive moduli.

Although the reported compressive moduli of the alginate hydrogels are relatively weak, the results are within the same order of magnitude (kPa) as those of alginate hydrogels reported previously.[31,36,39,40] A-P-9 hydrogels (0.40 (w/v %) Ca-0.12 (w/v %) P) exhibited the greatest strength among tested hydrogels of various calcium and phosphate compositions. This can be attributed to a greater number of alginate-calcium bonds formed at a higher calcium concentration. As previously mentioned, the highest phosphate concentration postponed the gelation process via precipitation with calcium ions. This allowed for controlled diffusion of the remaining calcium throughout the alginate before the ions contributed to gelation, which resulted in uniform hydrogels.

The addition of various weight percentages of pure collagen fibers did not significantly affect the gelation time of the alginate hydrogels. Also, the differences in time were not statistically significant from that of the control. However, the compressive moduli of the hydrogels with 2.5, 5 and 10 weight percents pure collagen fibers did significantly increase compared to the control (A-P-9). This can be attributed to the composite rule of mixtures which explains that the mechanical strength of a composite is in between those of the continuous, matrix phase and reinforcement phase.[41] As the compressive modulus of collagen fibers is greater than that of alginate, it is reasonable that the average compressive modulus of A-C hydrogels is greater than that of A-Ca hydrogels.

Figure 4 shows that the average gelation times of A-MC-1a and A-MC-1b hydrogels with 2.5 % (w/v) and 5 % (w/v) mineralized collagen fibers, respectively, were shorter than that of the control and the differences in times were statistically significant. The average gelation times were also significantly shorter than that of hydrogels with 2.5 % (w/v) pure collagen fibers. This

eludes to the fact that the mineralized fibers have an impact on the gelation rate of the alginate hydrogels.

Kikuchi et al. explain that the *in situ* formation of hydroxyapatite onto collagen fibers is initiated by the nucleation of calcium ions onto the carboxyl groups of the collagen fibers.[10,11] The calcium ions then bind to the phosphate ions added to the collagen solution, forming hydroxyapatite. This *in situ* nucleation process has been adapted in our m-SBF method to form apatite onto our collagen fibers (mineralized collagen fibers) before alginate addition. The particles deposited onto the collagen fibers are apparent in Fig. 3. This apatite precipitation technique has been extensively researched in our lab and hydroxyapatite formation onto collagen hydrogel fibers has been confirmed using various characterization analyses in previous studies.[15,42] Tampieri et al. have indicated that apatite particles could provide calcium ions capable of crosslinking alginate chains.[35] Lu et al. also suggested that *in situ*, calcium ions are released from apatite particles to aid in alginate gelation.[40] Thus, it is hypothesized that the apatite nucleated onto our collagen fibers can also release calcium ions into solution. The released calcium is then available to bind to the carboxyl groups of the alginate chains, resulting in premature partial crosslinking. In other words, the crosslinking of alginate G blocks occurred before the addition of $CaSO_4$. The proposed process is depicted in Fig. 10.

The proposed partial crosslinking of alginate chains before the addition of $CaSO_4$ is supported by the observed increase in viscosity and gelation rate of the alginate suspension with mineralized collagen fibers (A-MC-1) when compared to the pure alginate suspension. This also provides an explanation as to why the addition of pure collagen fibers to the alginate suspension resulted in a significant increase in compressive modulus while the addition of mineralized

collagen fibers in A-MC-1 hydrogels did not. Because the pure collagen fibers are not hindering the binding of the G blocks to the calcium, they are able to serve as reinforcements.

To further investigate the hypothesis that premature alginate crosslinking occurred, the order in which the constituents were added to form the hydrogel was modified so that the phosphate solution was added before the alginate powder (A-MC-2). Thus, any calcium released from the mineralized collagen fibers would precipitate with the phosphate ions to form calcium phosphate, which would prevent premature partial gelation of the alginate. This is supported by our experimental data as an increase in gelation time of the A-MC-2 hydrogels compared to that of A-MC-1 hydrogels was observed. Therefore, the calcium ions had more time to disperse throughout the suspension before gelation occurred, resulting in a more controlled, uniform gelation process. As previously explained, hydrogels with more homogenous material properties demonstrate higher mechanical properties than inhomogenous hydrogels. This was exhibited by the A-MC-2 hydrogels which had the strongest compressive modulus out of all of the hydrogel samples studied. It is proposed that this is because the G block-calcium crosslinks were no longer disrupted by the mineralized collagen fibers and the fibers were able to serve as reinforcements in the alginate matrix.

The order in which the phosphate is added to the system plays a crucial role in the resulting material properties. By modifying the order of phosphate addition, the 2.5 % (w/v) A-MC-2 demonstrates the highest compressive modulus and appropriate gelation time. As such, it was identified as the most promising candidate as an injectable hydrogel for bone tissue engineering. The A-MC-2 gelation time is within the time defined as an "ideal surgical time" of 5-30 minutes and its compressive modulus is deemed sufficient for the proposed non-load bearing applications. These may include maxillofacial reconstruction or reinforcement purposes

such as filling bone micro-fractures or osteoporotic bone to simply increase the rate of healing.[6,17,43,44] Injection of the hydrogel into areas of weakened bone may help restore bone density by promoting bone growth. New bone formation induced by the hydrogel will enhance the mechanical strength of the area and hopefully prevent further bone breakage and weakening. Additionally, the compressive modulus of the hydrogel has the potential to be increased even further with an increase in calcium concentration, resulting in an increase in alginate-calcium crosslinks. The compressive modulus would increase as long as the calcium is released slowly and a homogenous hydrogel is produced. Furthermore, because the biocompatibility of the alginate hydrogel should increase substantially with the presence of mineralized collagen fibers, it is a worthwhile addition to the system.

4.2 Characterization of Hydrogel Inorganic Composition

Thermogalvanic analysis (TGA) of the hydrogel samples after heating to 900 °C removed all of the organic components from the sample, leaving behind the inorganic residue. In this case, the inorganic components are calcium phosphate phases and sulfate salts, proven by XRD and FTIR analyses. The addition of phosphate to A-Ca hydrogels resulted in a statistically significant increase in weight percent residue. The addition of collagen to the A-P hydrogels did not significantly affect the weight percent residue after 900 °C as the same amount of salts are present in the composition of both A-P and A-C hydrogels. The percent residue also does not significantly change with the addition of mineralized collagen fibers (A-MC-1) to the A-P hydrogels. However, when phosphate was added before alginate to prevent premature gelation (A-MC-2), a significant increase in percent residue was observed. This could be attributed to the fact that an increase in calcium ions took part in the formation of calcium phosphates in A-MC-2

compared to that of the A-MC-1 hydrogels. In the A-MC-1 hydrogels, a high concentration of calcium released from mineralized collagen fibers may have accumulated in local areas, contributing to early gelation and formation of less homogenous hydrogels. In contrast, the calcium ions released from mineralized collagen fibers in A-MC-2 reacted with phosphate pre-added to the solution, which effectively prevented pre-mature gelation. As a result, an increase in inorganic residue was observed. Thus, only remaining calcium ions from $CaSO_4$ contributed to organic crosslinks with the alginate chains, forming a homogenous hydrogel.

XRD spectra show the change in composition of the alginate hydrogels as the result of the addition of phosphate, pure collagen and mineralized collagen fibers. The peaks of each hydrogel are relatively broad, indicating poorly crystalline samples. A slight shift in peaks may be present in the A-C and A-MC samples due to the addition of calcium phosphate phases. In the A-C hydrogels, phosphate has the capability of nucleating onto the collagen fibers and precipitating with calcium ions to form calcium phosphate. A-MC hydrogels have apatite present on the collagen fibers to begin with. The interaction between alginate and calcium phosphate may result in compression of the polymer matrix, leading to peak to shifts.[45] Pure hydroxyapatite exhibits characteristic peaks of the (211), (300) and (202) planes as three separate, sharp peaks.[46] These peaks are overlapped into a broad peak in the A-MC hydrogels. This broadness of the apatite peaks can be attributed to the *in situ* formation of apatite, suggesting that hydroxyapatite is nano-sized and of low crystallinity.[45,47] An increase in peak broadening is observed in the A-MC-2 spectrum due to the increase in the nano-sized inorganic components in the hydrogel. However, these characteristics closely resemble that of natural bone, making this composition suitable as a bone substitute.[5]

FTIR spectra of the various alginate hydrogels show that the main alginate carboxyl absorption bands are present in each sample yet are not in the same exact location for each type of hydrogel. The addition of phosphate to A-Ca hydrogels results in the shifting of these bands at 1595 cm^{-1} and 1410 cm^{-1} to higher wavelengths, also known as a blue shift. This suggests an interaction between the alginate and the calcium phosphate formed. The shift in the PO_4 bending and OH^- stretching bands also confirm the interaction.[32] A shift to higher wave numbers is also seen after the addition of pure collagen fibers. When comparing A-C and A-MC hydrogels, a shift to a slightly lower wave number, or red shift, is seen in most absorbance bands. As Teng et al. explained, this is indicative of an interaction between organic and inorganic phases in the sample, supporting the idea that the *in situ* formed apatite crystals are in fact bonding with the collagen and alginate components.[45]

5. Conclusions

A novel, biocompatible injectable hydrogel for bone tissue regeneration has been developed. The gelation time has been optimized so that the injectability of the system is appropriate in a surgical setting, rendering a less invasive method for bone repair compared to implantation of bone tissue engineered scaffolds. Utilizing our *in situ* collagen fiber mineralization method, we were able to produce an alginate hydrogel comprised of collagen and calcium phosphate, the two main components of natural bone, which was proven via numerous material characterization techniques. Thus, this injectable hydrogel system contains the components necessary to promote new bone growth and can be a promising biomaterial for bone repair and regeneration.

6. Acknowledgements

The authors would like to thank NSF grants (CBET-1133883, CBET-1347130, CBET 1339536 and CBET 1226018) and the NSF GK-12 program (0947869) for their support.

References

1. C. Rey, C. Combes, C. Drouet and M.J. Glimcher, *Osteoporosis Int.*, 2009, **20**, 1013-1021.

2. L.L. Hench, R.J. Splinter, W.C. Allen and T.K. Greenlee, *Biomed Mater Res*, 1971, **5**, 117-141.

3. E.B. Nery, K.L. Lynch, W.M. Hirthe and K.H. Mueller, *Periodont* 1975, **46**, 328-333.

4. R.Z. LeGeros, A. Chohayeb and A. Shulman, *J Dent Res*, 1982, **61**, 343.

5. R.Z. LeGeros, *Adv Dent Res*, 1988, **2**, 164-180.

6. W.E. Brown and L.C. Chow, *US Pat*., 4 518 430, 1985.

7. M. Lebourg, J. Suay Anton and J.L. Gomez Ribelles, *J Mater Sci: Mater Med*, 2010, **21**, 33-44.

8. I. Manjubala, S. Scheler, J. Bossert and K.D. Jandt, *Acta Biomater*, 2006, **2**, 75-84.

9. A.A. Al-Munajjed, J.P. Gleeson and F.J. O'Brien, *Stud Health Technol Inform*, 2008, **133**, 11–20.

10. M. Kikuchi, S. Itohv, S. Ichinose, K. Shinomiya and J. Tanaka, *Biomaterials*, 2001, **22**, 1705-1711.

11. A. Ficai, E. Andronescu, G. Voicu, C. Ghitulica, B.S. Vasile, D. Ficai and V. Trandafir, *Chemical Engineering Journal*, 2010, **160**, 794-800.

12. A.A. Al-Munajjed, N.A. Plunkett, J.P. Gleeson, T. Weber, C. Jungreuthmayer, T. Levingstone, J. Hammer and F.J. O'Brien, *J Biomed Mater Res B*, 2009, **90B**, 584-591.

13. H. Qu, Z. Xia, D. Knecht and M. Wei, *J Am Ceram Soc* 2008, **91**, 3211–3215.

.

14. Z. Xia, X. Yu and M. Wei, *J Biomed Mater Res B,* 2012, **100B**, 871–881.

15. Z. Xia, X. Yu, X. Jiang, H. Brody, D. Rowe and M. Wei, *Acta Biomater*, 2013, **9**, 7308-7319.

16. S. Fu, P. Ni, B. Wang, B. Chu, L. Zheng, F. Luo, J. Luo and Z. Qian, *Biomaterials*, 2012, **33**, 4801-4809.

17. G. Ma, Q. Li, K. Wang, C. Binling, J. Kennedy and J. Nie, Carbohydrate Polymers, 2010, **79**, 620-627.

[18] C. Bucke, *Methods Enzymol.*, 1987, **135**, 175-189.

19. B.M. Watson, F.K. Kasper, P.S. Engel and A.G. Mikos, *Biomacromolecules*, 2014, **15**, 1788-1796.

20. D.F. Coutinho, S.V. Sant, H. Shin, J.T. Oliveira, M.E. Gomes, N.M. Neves, A. Khademhosseini and R.L. Reis, *Biomaterials*, 2010, **31**, 7494-7502.

21. D. McHugh in *Production and Utilization of Products from Commercial Seaweeds*, FAO Fisheries Technical Paper, Food and Agriculture Organization of the United Nations, Rome, Italy,1987, ch. 2.

22. J. Sun and H. Tan, *Materials*, 2013, **6**, 1285-1309.

23. A. Martinsen, G. Skjak-Braek and O. Smidsrod, *Biotechnol Bioeng*, 1989, **33**, 79-89.

24. R. Yao, R. Zhang, F. Lin and J. Luan, *Biotechnol Bioeng*, 2013, **110**, 1430-1443.

25. S. Sotome, T. Uemura, M. Kikuchi, J. Chen, S. Itoh, J. Tanaka, T. Tateishi and K. Shinomiya, *Materials Science and Engineering C*, 2004, **24**, 341–347.

26. T. Andersen, B.L. Strand, K. Formo, E. Alsberg and B.E. Christensen, *Carbohydr. Chem.*, 2012, **37**, 227-258.

27. G.T. Grant, E.R. Morris, D.A. Rees, P. Smith and D. Thom, *FEBS Letters*, 1973, **32**, 195-198.

28. R. Brayner, T. Coradun, F. Fievet-Vincent, J. Livage, and F. Fievet, *New J. Chem.*, 2005, **29**, 681–685.

29. I. Braccini, R.P. Grasso and S. Perez, *Carbohydr Res*, 1999, **317**, 119-130.

30. S.H. Cho, S.M. Lim, D.K. Han, S.H. Yuk, G.I. Im and J.H. Lee, *J Biomater Sci, Polym Ed.*, 2009, **20**, 863-876.

31. C.K. Kuo and P.X. Ma, *Biomaterials*, 2001, **22**, 511-521.

32. P. Parhi, A. Ramanan and A.R. Ray, *J Appl Polym Sci*, 2006, **102**, 5162–5165.

33. W. Li, P. Zhao, C. Lin, X. Wen, E. Katsanevakis, D. Gero, O. Felix and Y. Liu, *Biomacromolecules*, 2013, **14**, 2647-2656.

34. H.H. Jin, C.H. Lee, W.K. Lee, J.K. Lee, H.C. Park and S.Y. Yoon, *Materials Letters*, 2008, **62**, 1630–1633.

35. A. Tampieri, M. Sandri, E. Landi, G. Celotti, N. Roveri, M. Mattioli-Belmonte, L. Virgili, F. Gabbanelli and G. Biagini, *Acta Biomater*, 2005, **1**, 343–351.

36. R. Tan, X. Niu, S. Gan and Q. Feng, *J Mater Sci: Mater Med.*, 2009; **20**, 1245–1253.

37. S.M. Zhang, F.Z. Cui, S.S. Liao, Y. Zhu and L. Han, *J Mater Sci: Mater Med.*, 2003, **14**, 641-645.

38. N. Rajan, J. Habermehl, M.F. Coté, C.J. Doillon and D. Mantovani, *Nat Protoc*., 2007, **1**, 2753–2758.

39. M.A. LeRoux, F. Guilak and L.A. Setton, *J Biomed Mater Res*, 1999, **47**, 46-53.

40. L. Lu, Y.S. Qi, C.R. Zhou and Y.P. Jiao, *Sci China Tech Sci.*, 2010, **53**, 272−277.

41. J.Y. Rho, L. Kuhn-Spearing and P. Zioupos, *Medical Engineering and Physics*, 1998, **20**, 92-102.

42. Z. Xia, M.M. Villa and M. Wei, *J. Mater. Chem. B*, 2014, **2**, 1998- 2007.

43. Z. Noor, *Journal of Osteoporosis*, 2013, **2013**, 1-6.

44. S.C.N. Chang, J.A. Rowley, G. Tobias, N.G. Genes, A.K. Roy, D.J. Mooney, C.A. Vacanti and L.J. Bonassar, *J Biomed Mater Res.*, 2001, **55**, 503-511.

45. S. Teng, J. Shi, B. Peng and L. Chen, *Composites Science and Technology*, 2006, **66**, 1532-1538.

46. E.R. Kramer, A.M. Morey, M. Staruch, S.L. Suib, M. Jain, J.I. Budnick and M. Wei, *J Mater Sci*., 2013, **48**, 665-673.

47. L. Wang, Y. Li and C. Li, *J Nanopart Res,* 2009, **11**, 691-699.

Table 1: Compositions of A-Ca and A-P hydrogels

Hydrogel	Alginate Final % (w/v)	$CaSO_4$ Final % (w/v)	Na_2HPO_4 Final % (w/v)
A-Ca-1	1.5	0.20	0
A-Ca-2	1.5	0.30	0
A-Ca-3	1.5	0.40	0
A-P-1	1.5	0.20	0.04
A-P-2	1.5	0.30	0.04
A-P-3	1.5	0.40	0.04
A-P-4	1.5	0.20	0.08
A-P-5	1.5	0.30	0.08
A-P-6	1.5	0.40	0.08
A-P-7	1.5	0.20	0.12
A-P-8	1.5	0.30	0.12
A-P-9	1.5	0.40	0.12

Table 2: Composition of A-C and A-MC hydrogels

Hydrogel	Alginate Final % (w/v)	$CaSO_4$ Final % (w/v)	Na_2HPO_4 Final % (w/v)	Pure Collagen Fiber Final % (w/v)	Mineralized Collagen Fiber Final % (w/v)
A-C-1	1.5	0.40	0.12	2.5	0
A-C-2	1.5	0.40	0.12	5.0	0
A-C-3	1.5	0.40	0.12	10.0	0
A-C-4	1.5	0.40	0.12	20.0	0
A-MC-1a	1.5	0.40	0.12	0	2.5
A-MC-1b	1.5	0.40	0.12	0	5.0
A-MC-2*	1.5	0.40	0.12	0	2.5

*Phosphate solution was added to mineralized collagen suspension before the addition of alginate powder

Table 3: Compositions of selected hydrogels for characterization of inorganic content

Hydrogel	Alginate % (w/v)	$CaSO_4$ % (w/v)	Na_2HPO_4 % (w/v)	Collagen Fibers % (w/v)	Mineralized Collagen Fibers % (w/v)
A-Ca-1: Alginate-CaSO4	1.5	0.20	0	0	0
A-P-9: Alginate-Phosphate	1.5	0.40	0.12	0	0
A-C: Alginate-Collagen	1.5	0.40	0.12	2.5	0
A-MC-1: Alginate-Mineralized Collagen	1.5	0.40	0.12	0	2.5
A-MC-2: Alginate-Mineralized Collagen	1.5	0.40	0.12	0	2.5

Figure 1: Suspension (left) and gel (right) states of alginate hydrogels
36x20mm (600 x 600 DPI)

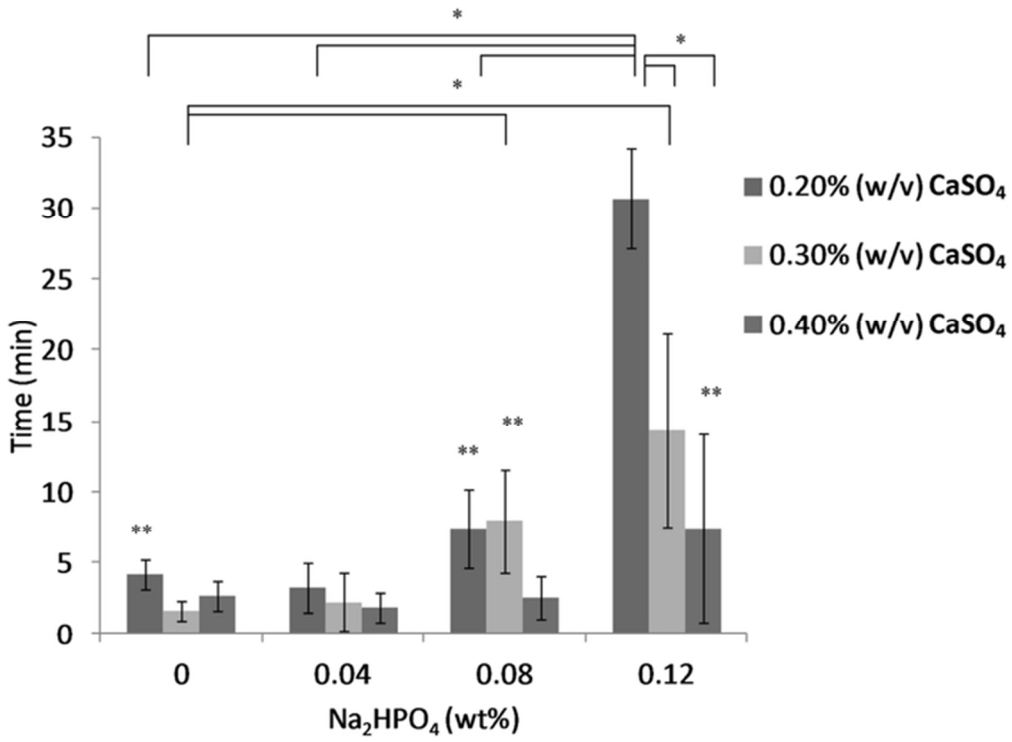

Figure 2 : Average gelation times of alginate hydrogels with varying Na_2HPO_4 and $CaSO_4$ concentrations. *Statistically significant from each other ($p < 0.05$, ANOVA) **Selected compositions for mechanical testing 29x21mm (600 x 600 DPI)

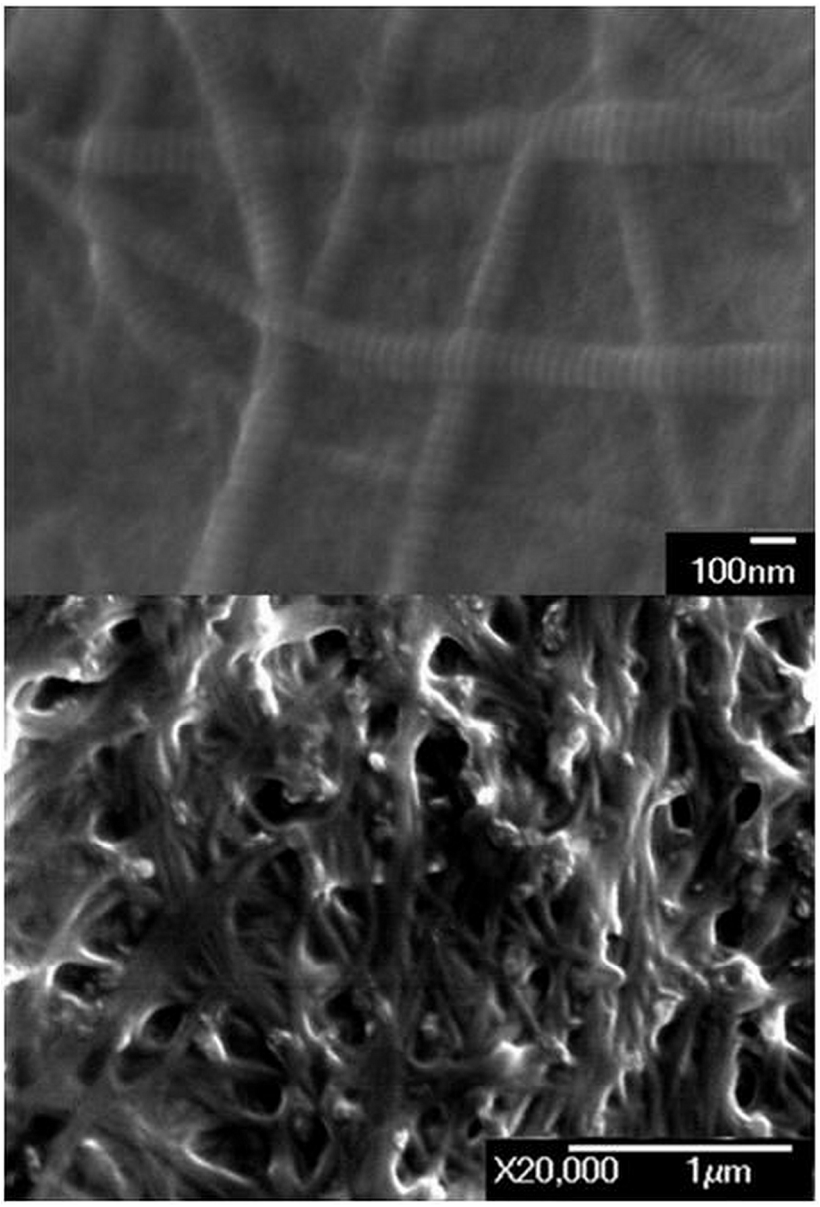

Figure 3: FESEM images of air dried a) pure collagen fibers and b) mineralized collagen fibers
59x87mm (600 x 600 DPI)

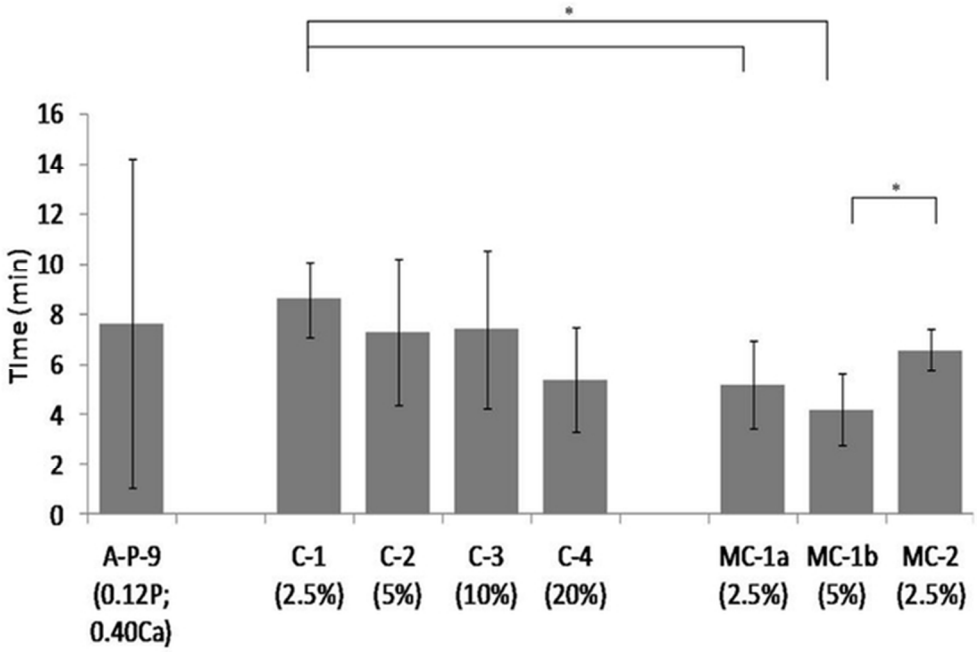

Figure 4: Gelation times of alginate hydrogels with varying pure collagen (C) or mineralized collagen (MC) fiber content *Statistically significant from each other ($p < 0.05$, ANOVA)
28x19mm (600 x 600 DPI)

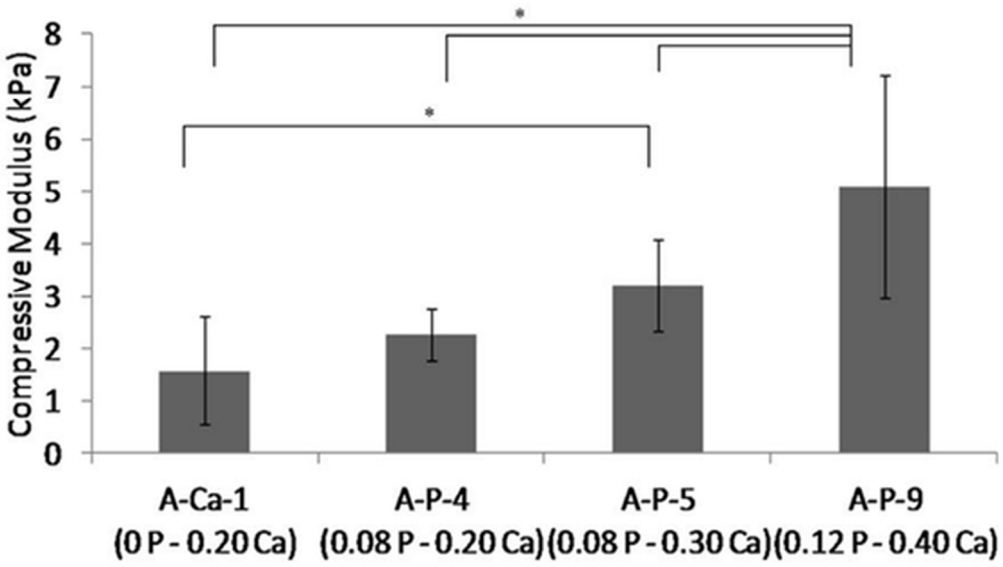

Figure 5: Compressive moduli of alginate hydrogels of varying Na_2HPO_4 and $CaSO_4$ contents *Statistically significant from each other ($p < 0.05$, ANOVA)
23x13mm (600 x 600 DPI)

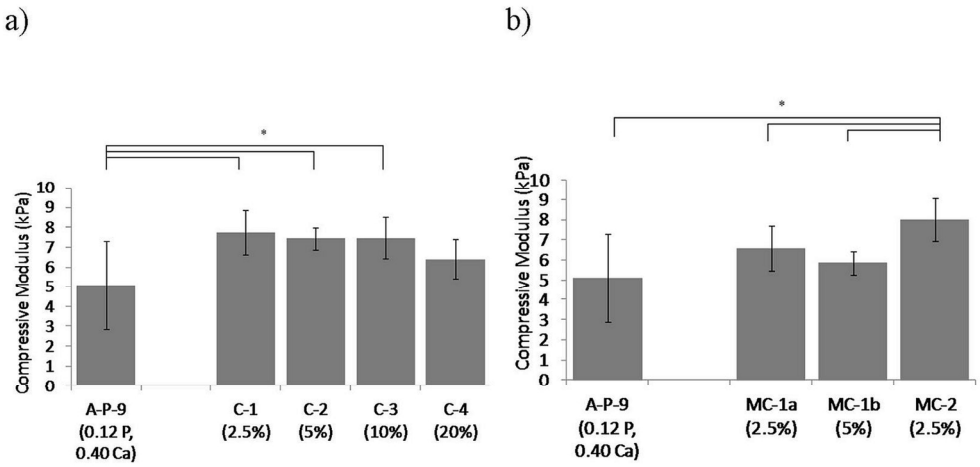

Figure 6: Compressive moduli of various a) A-C and b) A-MC hydrogels *Statistically significant from each other ($p < 0.05$, ANOVA)
77x38mm (600 x 600 DPI)

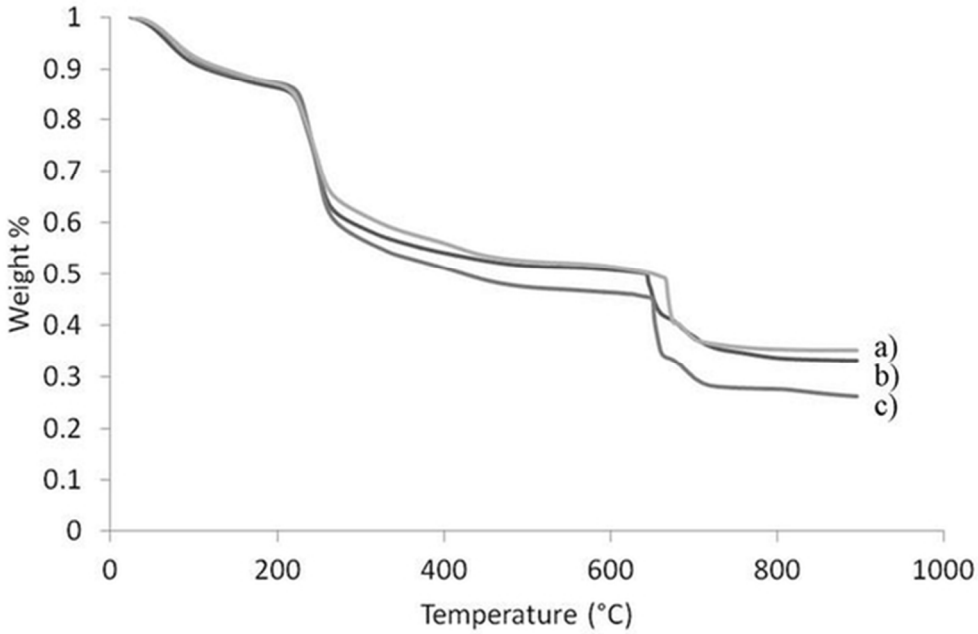

Figure 7: TGA curves of alginate hydrogels containing a) A-MC-2, b) A-P-9 (0.40 % Ca-0.12 % P) and c) A-Ca-1 (0.20 % Ca-0 % P)
26x17mm (600 x 600 DPI)

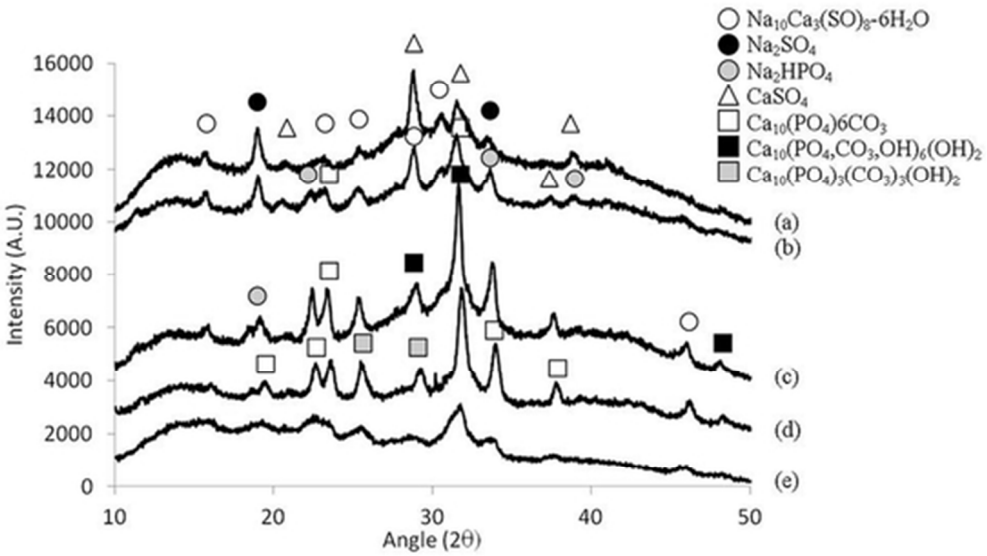

Figure 8: XRD patterns of (a) A-Ca-1, (b) A-P-9, (c) A-C-1, (d) A-MC-1a and e) A-MC-2 hydrogels
23x13mm (600 x 600 DPI)

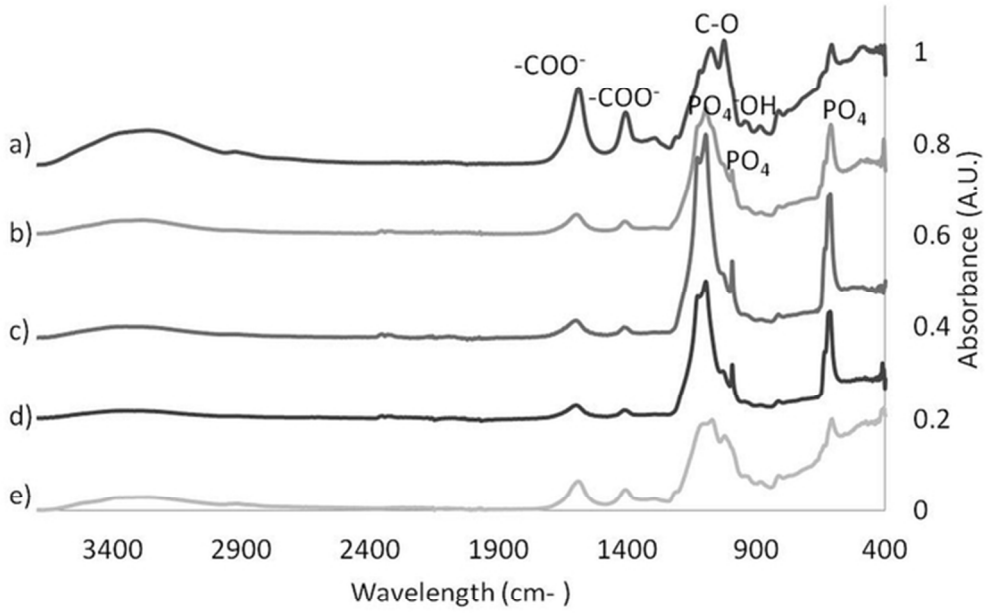

Figure 9: FTIR spectra of (a) A-Ca-1 (b) A-P-9, (c) A-C-1, (d) A-MC-1a and e) A-MC-2 hydrogels
28x20mm (600 x 600 DPI)

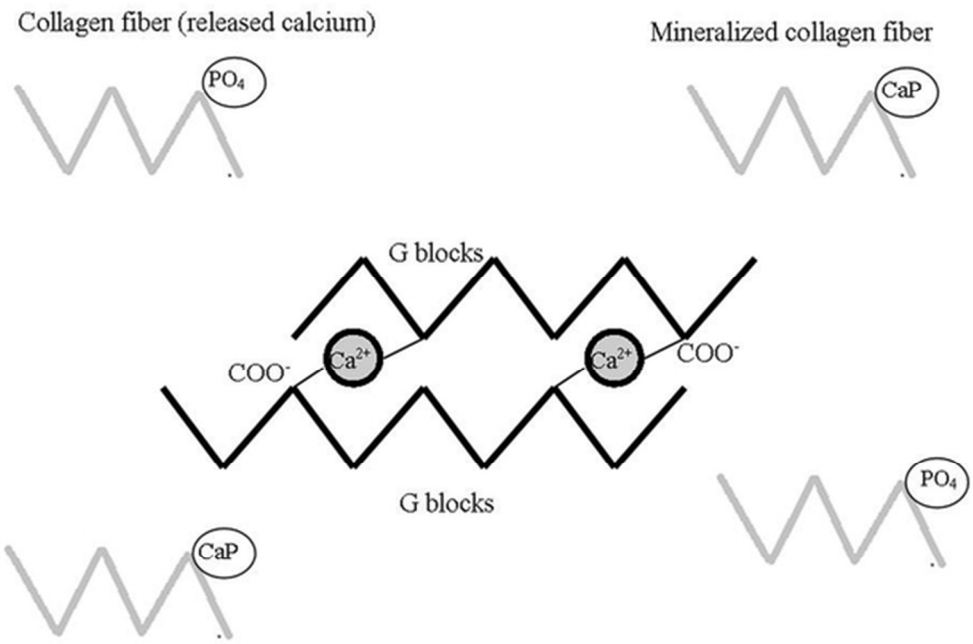

Figure 10: Schematic of the hypothesized "pre-mature" alginate crosslinking mechanism
26x17mm (600 x 600 DPI)

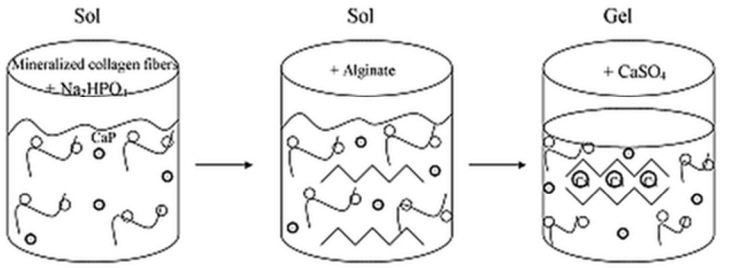

This novel fabrication process allowed for the development of an injectable hydrogel system with a gelation time suitable for a surgical setting and components necessary for promoting enhanced bone regeneration

This novel fabrication process allowed for the development of an injectable hydrogel system with a gelation time suitable for a surgical setting and components necessary for promoting enhanced bone regeneration.
31x24mm (600 x 600 DPI)